HHS Public Access

Author manuscript

Drug Discov Today. Author manuscript; available in PMC 2018 September 01.

Published in final edited form as:

Drug Discov Today. 2017 September ; 22(9): 1421–1429. doi:10.1016/j.drudis.2017.04.008.

Next Generation Superparamagnetic Iron Oxide Nanoparticles for Cancer Theranostics

Kai Li[*], **Hossein Nejadnik**, and **Heike E. Daldrup-Link**[*]

Department of Radiology and Molecular Imaging Program at Stanford (MIPS), Stanford School of Medicine, Stanford, CA

Abstract

Superparamagnetic nanoparticles of iron oxides (SPIO) have been intensively studied for the development of contrast agents in magnetic resonance imaging (MRI). First generation SPIO had diagnostic capabilities only, while a new generation of SPIO have multifunctional characteristics for combined therapeutic and diagnostic applications. These theranostic nanoparticles hold great potential for image-guided cancer therapies. Especially, polymer-coated theranostic SPIO have enjoyed increasing attention due to good biocompatibility, biodegradability and versatile functionality endowed by polymeric matrices. This review provides an overview of recently developed polymer-coated multifunctional SPIO for cancer theranostics and discusses current challenges and future perspectives.

Keywords

Superparamagnetic nanoparticles of iron oxides; magnetic resonance imaging; cancer theranostics; multifunctional nanoparticles; polymer-coated nanoparticle

Introduction

There are approximately 4,600 new cancer diagnoses each day and cancer is the second leading cause of death in the United States [1]. Early and sensitive cancer diagnosis along with effective treatment are critical for favorable outcomes. Superparamagnetic iron oxide (SPIO) nanoparticles have been successfully used for staging and treatment monitoring of a variety of cancers with magnetic resonance imaging (MRI) [2,3]. Since imagers have successfully delivered SPIO to cancers through intravenous injection [4-6], we can build on decades of this experience and use these same probes as Trojan horses for the delivery of therapeutic drugs to cancers.

First generation SPIO are relatively easy to synthesize, have high r_1 and r_2 relaxivities and can be completely eliminated from the body [7,8]. SPIO accumulate in cancer through passive targeting by the enhanced permeability and retention (EPR) effect or through active targeting with the help of targeting ligands [9-11]. The magnetite (Fe_3O_4) and maghemite

[*]Corresponding authors: Dr. H.E. Daldrup-Link (H.E.Daldrup-Link@stanford.edu); Dr. K. Li (kai2@stanford.edu), Phone: +1-650-723-8996.

Conflicts of interest: The authors declare that they do not have any conflicts of interest.

(Fe_2O_3) cores of SPIO can be readily detected with MRI, thereby enabling real-time *in vivo* drug tracking. To provide colloidal stability of the magnetic core and better biocompatibility, SPIO have been stabilized with polysaccharides (e.g., dextran and chitosan), polyethylene glycol (PEG), polypyrrole (PPy), polylactic acid (PLA), poly(D,L-lactic-*co*-glycolic acid) (PLGA) and their copolymers. Compared to other coating materials such as silica, polymers enjoy advantages in good biocompatibility and biodegradability.

New generation SPIO combine diagnostic and therapeutic capabilities in a single formulation [12,13]. A schematic illustration of multifunctional theranostic SPIO is shown in Fig. 1. The polymer coating of SPIO can be loaded with therapeutic agents to facilitate MRI guided drug delivery, gene delivery, photothermal therapy (PTT), photodynamic therapy (PDT) or magnetic hyperthermia. Cancer specificity can be further increased by using “smart” polymers for controlled drug release in response to external stimuli, such as pH, temperature or tumor enzymes.

While previous investigators reviewed the synthesis and application of SPIO in biomedical imaging [14-17], this short review will provide an overview of recently developed, new generation multifunctional SPIO for cancer theranostics over the past 2-3 years (since 2014). Special attention is paid on “smart” and activatable probes. We also discuss current challenges and future perspectives with the goal to inspire new research opportunities and facilitate clinical translation.

SPIO-delivered chemotherapy

A variety of chemotherapeutic agents have been incorporated into SPIO-based nanocarriers through different strategies (e.g., conjugation via cleavable linker and **π**-**π** stacking with polymer layers) for delivery to tumors [18,19]. All of these chemotherapeutic drugs have in common low molecular weights, rapid biodistribution and elimination from the body. Attaching these small molecules to SPIO increases their blood circulation half-life, promotes their tumor retention through the EPR effect and enables real-time *in vivo* drug tracking with MRI [20]. Although SPIO nanoparticles are normally metabolized in the liver, they were also found to accumulate in other organs of the reticuloendothelial system (e.g., spleen) [21,22], where the drug conjugates can exert potential toxic effects especially after multiple dose administration. To minimize off-target toxicity of SPIO-conjugated cytotoxic drugs to normal organs, several design principles have been employed, including pH-, temperature- and enzyme-mediated drug release in tumors.

Inspired by pH differences in blood and tumors, pH-responsive polymeric nanosystems have been developed to minimize cytotoxic drug release in blood and maximize pH-dependent activation in tumors [23,24]. Zhang *et al.* coated SPIO with methoxypoly(ethylene glycol)-*b*-poly(2-(dimethylamino) ethyl methacrylate)-*b*-poly(glycerol monomethacrylate) (MPEG-*b*-PDMA-*b*-PGMA) and attached cisplatin by coordinating amine groups in PDMA with Pt atoms in cisplatin [25]. Cumulative release of cisplatin from the theranostic SPIO was ~36% in acidic environment (pH 5.7) compared to 22% in neutral environment (pH 7.4). This pH-dependent release profile can be attributed to the protonation of amine groups in PDMA segments at lower pH, which compromised their coordination ability and led to cisplatin

release. Investigators added folate-poly(ethylene glycol)-*b*-poly(glycerol monomethacrylate) (FA-PEG-*b*-PGMA) in the encapsulation matrix to obtain additional FA-PEG shells, which enabled cancer targeting ability and antifouling property. *In vitro* studies showed improved cytotoxicity of cisplatin-loaded and folate-conjugated SPIO to Hela cells compared to the original theranostic SPIO, due to the specific targeting effect of folate to Hela cells with higher internalization efficiency.

Vivek *et al.* reported the synthesis of pH-responsive theranostic SPIO, composed of Fe_3O_4 as a core and PLGA as a shell [26]. PLGA is a biocompatible and biodegradable polymer coating for theraostic SPIO, which is approved by Food and Drug Administration (FDA) and thereby, enables translational drug development [27]. The PLGA shell was loaded with the anticancer drug, tamoxifen (TAM) and surface targeting ligands (Herceptin) with specific binding affinity to human epidermal growth factor receptor-2 (Her-2). The resultant theranostic SPIO showed no significant TAM release at pH 7.4 (“Off” state), but polymer degradation, TAM release in the acidic environment (pH 5.0) in *in vitro* tests (“On” state). This feature suggests the potential of such PLGA-encapsulated SPIO for targeted cancer cell toxicity upon internalization by Her-2-overexpressed cells through endocytosis, which triggers pH-dependent drug release in late endo/lysosome with acidic environment.

Other investigators took advantage of the temperature-responsive function of poly(*N*-isopropylacrylamide) (PNIPAM): Wang *et al.* synthesized PNIPAM-based multifunctional nanogels for simultaneous optical temperature sensing, tumor cell imaging and magnetic/near-infrared (NIR)-induced drug release [28]. The hybrid nanogels were prepared by coating bifunctional SPIO (SPIO clusters covered by porous carbon shell containing fluorescent carbon dots) with a PNIPAM copolymer, poly(*N*-isopropylacrylamide-*co*-acrylamide) and cancer therapeutic curcumin. With increasing temperature, the fluorescence of the nanogels increased due to contraction of the PNIPAM layer with decreased surface trap states acting as emission quenching centers. The nanogels also exhibited temperature-dependent curcumin release (35.3% and 70.4% at 37 °C and 41 °C, respectively) and cytotoxicity against B16F10 cells. At high temperature, the contraction of PNIPAM coating above lower critical solution temperature (LCST) can squeeze out the curcumin molecules quickly from the shell and reduce the diffusion path of drug molecules. The temperature-dependent drug release from PNIPAM can be further augmented by applying NIR light or alternating magnetic fields (AMF) because the carbon layer can absorb and convert NIR light to heat and the SPIO core can generate heat in AMF. Other research group also showed that AMF increased the temperature of PNIPAM coated theranostic SPIO and accelerated the release of the anti-cancer drug 5-fluorouracil [29].

Another effective way to reduce side effects of chemotherapy is to design nontoxic prodrugs that are mainly activated in the tumor tissue but not healthy organs. This can be achieved by linking SPIO and cytotoxic drugs so that the therapeutic drug is inactive when attached to SPIO and activated when released. The linker can be tumor enzyme-cleavable peptide.

Since lysosomal proteases are abundant in tumor cells but not healthy organs [30], Lin *et al.* designed protease-mediated drug release systems [31]. The cytotoxic drug methotrexate (MTX) was attached to PEG and chitosan-coated SPIO via a protease-cleavable amide

linker. The structural similarity between MTX and folate enabled cellular uptake into folate receptor-overexpressing Hela cells and intracellular proteases mediated drug release. Ansari *et al.* conjugated the highly cytotoxic drug azademethylcolchicine (ICT) to the dextran layer of the SPIO ferumoxtol using a peptide linker, which can be cleaved by matrix metalloproteinase-14 (MMP-14) [32]. The drug (CLIO-ICT) caused significant apoptosis of MMP-14 expressing tumor cells *in vitro* and *in vivo*, in MMTV-PyMT tumor-bearing mice, without collateral toxicity to non-MMP-14 expressing cells and normal organs (Fig. 2).

It is important to note that SPIO (without attached cytotoxic drugs) have intrinsic therapeutic effects: ferumoxytol can inhibit cancer growth by inducing a pro-inflammatory immune response with M1 macrophage polarization [33]. Therefore, investigation of SPIO-based theranostics needs to include studies of the original SPIO, original cytotoxic drug and combined drug, in order to understand and optimize effects of each drug component in the tumor microenvironment.

SPIO-mediated gene therapy

Conventional chemotherapy kills rapidly dividing cells in both tumors and normal tissues. Since most cancers have abnormal gene expression profiles, cancer-targeted therapies have been developed to specifically block these genes or downstream molecular target [34,35]. For instance, delivery of therapeutic DNA can replace defective genes and regulate specialized protein expression to kill cancer cells [36,37]. Alternatively, RNA interference (RNAi) using small interfering RNA (siRNA) or microRNA (miRNA) can suppress expression or translation of cancer-promoting genes efficiently [38]. SPIO can help deliver therapeutic DNA and RNA to tumors. Since DNA/RNA biomolecules are fragile and sensitive to enzymes, it is essential to protect them from degradation during their transportation to tumors. A common method is to use cationic polymers that can encapsulate or bind negatively charged DNA/siRNA through electrostatic interaction [39]. Another approach is to chemically link biotherapeutic agents to nanocarriers through disulfide bonds that are cleaved by intracellular glutathione to release the biomolecules [40], which facilitates specific intracellular release.

Wang *et al.* used SPIO coated with chitosan-PEG grafted polyethyleneimine (CS-PEI) as nanovectors for the delivery of targeted siRNA to orthotopic hepatocellular carcinoma (HCC) xenografts in a mouse model [41]. The negatively charged Luc gene-targeting siRNA was loaded to polymer-coated SPIO through electrostatic interaction with PEI segments. PEG linkers were further immobilized on the surface to protect siRNA and facilitate conjugation with antibody against human glypican-3 (GPC3) receptor. Upon intravenous injection, the GPC3 Ab-functionalized siRNA nanovectors showed specific targeting ability to HCC and significantly suppressed Luc expression of the tumor, demonstrating the potential of such nanovectors for targeted delivery of therapeutic siRNA to HCC. In another study, Hernández-Gil *et al.* incorporated a Pt(IV) prodrug of cisplatin and a dsRNA analog, poly (I:C) into SPIO, which greatly enhanced the secretion of IL-12 of bone marrow-derived dendritic cells for targeted chemoimmunotherapy [42].

A major limitation of above mentioned molecularly targeted cancer therapy approaches is the complex and adaptive nature of cancers, which may contain hundreds of genetic variants [43]. A randomized trial of targeted therapy based on molecular profiling for advanced cancers from diverse anatomical locations showed no improvement in progression-free survival [44]. The NCI-Molecular Analysis for Therapy Choice (NCI-MATCH) trial, which links cancer patients with targeted drugs against their cancer DNA mutations, matched less than 5% of screened patients to a personalized trial thus far. Therefore, even if effective, this approach is expected to help only a small minority of cancer patients [45]. Future approaches need to target a broad set of cancer genes and may benefit from combinations with other therapies.

SPIO-delivered photothermal therapy

Photothermal therapy (PTT) uses near infrared irradiation (NIR) laser irradiation to generate heat for tumor ablation [46]. Compared to conventional therapeutic approaches, PTT can provide more precise spatial-temporal selectivity with little collateral damage of adjacent normal tissues [47]. This feature is most useful for non-metastasized and non-resectable cancers in critical anatomical locations, such as the brain. Various NIR-absorbing materials including gold nanomaterials, carbon nanomaterials and semiconducting polymers can amplify the conversion of absorbed photon energy into heat and kill localized tumor cells. SPIO can act as effective nanocarriers to deliver the PTT agents to tumor sites for imaging guided therapeutic treatment.

Zhang *et al.* encapsulated SPIO, gold nanoparticles and paclitaxel (PTX) in PEO-*b*-PCL copolymer through a flash nanoprecipitation approach [48]. The resultant PTX-Au-IO nanoparticles provided concurrent chemotherapy and PTT. The authors found significant toxicity to MCF-7 and MDA-MB-231 cells at 72 h after PTX-Au-IO treatment and further increased cell death at 5 min after laser irradiation due to photothermal effect. The SPIO core of the drug could be localized with MRI. As Au is also a good candidate for CT, researchers synthesized a star-shaped Au-coated Fe_3O_4 with PEI and PEG-folate coating for targeted trimodal imaging (MRI/CT/PAI) guided PTT in Hela tumor-bearing mice [49].

Hu and co-workers reported a new class of activatable theranostic nanocomposites for combined gene therapy and photothermal therapy (PTT) [50]. They linked negatively charged polydopamine (PDA)-coated Fe_3O_4 and positively charged poly(2-dimethyl amino)ethyl methacrylate (PDM)-coated Au nanorods (Au NR), producing positively charged Au/Fe_3O_4 which efficiently bound plasmid DNA (plasmid p53), a tumor suppressor gene to inhibit tumor cell proliferation. In the reducing tumor environment, the disulfide bonds in the PDM copolymer were cleaved and p53 was released. The Au/Fe_3O_4 core allowed non-invasive *in vivo* drug tracking with computed tomography (CT) and MRI. Additionally, the combined NIR absorbance properties of Au/Fe_3O_4 enabled photoacoustic imaging (PAI) and PTT. Upon intratumoral injection of the p53-decorated Au/Fe_3O_4 nanopcomposites into subcutaneous glioma xenografts in mice and NIR laser irradiation to the tumor sites, significant tumor necrosis and growth inhibition were achieved with combined PTT and gene therapy. Noteworthy is that PTT itself without p53 gene could induce efficient tumor ablation at the early treatment but the tumor started to grow in the

following days due to the rapid proliferation of C6 glioma, indicating the importance of combined PTT and gene therapy to suppress tumor growth in a long term.

Besides inorganic Au, NIR absorbing semiconducting polymers such as PPy received significant attention for PTT strategies [51]. Song *at al.* coated SPIO with PEG and PPy through a layer-by-layer approach for MRI and PAI guided PTT [52]. 4T1 tumors in BALB/c mice showed significant IONP@PPy-PEG accumulation at 24 h post intravenous injection, as confirmed by *in vivo* bimodal MRI and PAI, and response to 808 nm laser irradiation. The mice were tumor-free after treatment without noted side effect or organ damage within 40 days. The same group also integrated doxorubicin (DOX) chemotherapy into a similar platform to afford Fe_3O_4@PPy-PEG-DOX nanoparticles [53]. The aromatic doxorubicin molecules were loaded through hydrophobic interaction and **π-π** stacking with PPy layers. With an 808 nm NIR laser irradiation, PPy exhibited strong PTT effect and accelerated release of DOX at pH 5.0 and 6.0, owing to the protonation of amine groups in the DOX molecules at acidic pH and the increased thermal vibration of PPy chains that weakened the binding with DOX. Noteworthy is that the NIR laser could not promote drug release under physiological pH 7.4, suggesting the drug release only happens under NIR exposure after entering cancer cell endosomes and lysosomes with minimized side effect in circulation. T_2-weighted MR images showed that a strong darkening effect in the tumor area was observed after injection with Fe_3O_4@PPy-PEG-DOX for imaging-guided cancer therapy (Fig. 3a). The combination of PTT and chemotherapy offered by Fe_3O_4@PPy-PEG-DOX under laser irradiation was the most effective and resulted in complete elimination of most tumors (Fig. 3b-e).

SPIO-delivered photodynamic therapy

Photodynamic therapy (PDT) utilizes photosensitizing agents, which generate toxic reactive oxygen species (ROS) after exposure to light at a specific wavelength [54]. Similar to PTT, PDT provides high spatial-temporal accuracy. Therefore, PDT may offer a treatment option for patients with locally recurrent and non-metastasized cancer that is not responding to conventional therapies [55]. Fluorescent photosensitizers can be imaged with optical imaging approaches. Adding SPIO facilitates tumor retention and enables drug tracking with MRI.

Wang *et al.* reported a multifunctional drug delivery system which utilized red blood cells (RBCs) as Trojan horses [56]. First, SPIO were coated with chlorine e6 (Ce6) and RBCs were loaded with DOX. IONP-Ce6 and DOX-loaded RBCs were then connected through biotin-avidin specific binding and stabilized with PEG. Compared to IONP-Ce6-PEG, the DOX@RBC-IONP-Ce6-PEG showed prolonged blood circulation half-life, reduced retention in spleen and liver and enhanced tumor-homing ability after magnetic targeting with magnets attached to the tumor sites. Subsequent PDT (660 nm light irradiation for 2 h) significantly suppressed tumor growth by ~90% compared to single PDT with RBC-IONP-Ce6-PEG (no DOX, 57%) or single chemotherapy with DOX@RBC-IONP-Ce6-PEG (no light, 38%).

SPIO-induced magnetic hyperthermia

In the presence of an external magnetic field, the inherent magnetic properties of SPIO can induce localized hyperthermia due to Néel and Brownian relaxation effects [57]. At temperatures above 42 °C, cancer cells develop structural and functional damage (e.g., damage of protein, membrane and cytoskeletons) which can lead to apoptosis [58]. In addition to direct effects on cancer cells, hyperthermia can destabilize cancer cells and make them more vulnerable to chemotherapy or radiotherapy [59].

Quinto and colleagues reported phospholipid-PEG-coated SPIO as nanocarriers for drug delivery and hyperthermia treatment to Hela cells [60]. DOX was loaded into phospholipid-PEG layers through electrostatic interaction with the negatively charged phosphate groups in phospholipid segments. Longer PEG segments yielded lower DOX loading efficiency, probably because longer PEG chains shielded the phosphate groups more effectively. On the contrary, the PEG length had minimal influence on the heating efficiency of SPIO. After exposure to AMF for 20 minutes, the solution of DOX-SPIO reached a temperature of 43 °C and they were capable to induce significantly increased death of Hela cells compared to either DOX or SPIO treatment alone.

Zhou *et al.* developed a nanocomposite, Fe_2O_3@PPy-DOX-PEG, with PPy coating and DOX loading [61]. The cubic nanoporous Fe_2O_3 demonstrated pH-dependent and hyperthermia-induced DOX release *in vitro* and significant growth suppression of HepG2 tumor in nude mice after treatment with AFM for 45 min. In addition, the Fe_2O_3 core enabled *in vivo* drug tracking with MRI.

Conclusion and prospects

SPIO play an important part in the development of multifunctional and activatable theranostics for cancer patients. SPIO may shuttle cytotoxic drugs, DNA and RNA into tumors, and serve as mediators for PTT, PDT and magnetic hyperthermia (Table 1). Novel “smart” and activatable formulations may improve cancer specific therapeutic effects and spare normal organs from toxic side effects. Innovative theranostic SPIO have shown promising results in murine models, but translational efforts are lacking. While some SPIO formulations have been approved by the FDA (e.g., Feraheme® and Feridex I.V.®,) not a single functionalized SPIO has been approved for use in patients to date. This may be in part driven by an academic system, which rewards the development of ever new formulations with high impact publications and related academic rewards while clinical development of existing formulations is considered unoriginal and as a consequence, less worthwhile to pursue. As a community, we have to address this problem and develop processes that support the validation and clinical development of novel promising theranostics.

The impact of a variety of parameters, such as biocompatibility, colloidal stability and biodegradability on human biological responses must be comprehensively tested and understood before promising products can be further developed. In case of activatable SPIO, both the prodrug and the cleaved products need to be studied. In addition, potential toxic side effects of added components such as Au and PPy should be carefully examined.

Another major challenge in translational research is the feasibility and consistency to produce multifunctional SPIO in a large scale. The standardization and scalable production of SPIO remain a concern for clinical development and commercialization. In spite of these challenges, new generation of SPIO holds great potential for personalized medicine. Additionally, besides organic/inorganic hybrid nanoparticles based on SPIO, a variety of nanoparticles (e.g., pure organic nanoparticles) have also been intensively used for cancer theranostics, including drug delivery, PTT, PDT, fluorescence imaging and photoacoustic imaging, which will inspire more research interest in future. Intense interdisciplinary research crossing nanotechnology, material sciences, cancer biology and clinical medicine along with a focus on clinical translation will ultimately lead to tangible benefit for our patients.

Acknowledgments

Our SPIO research work is supported by a grant from the National Cancer Institute (NCI), grant number R21CA190196, two grants from the National Institute of Arthritis and Musculoskeletal and Skin Diseases (NIAMS), grant number R21AR066302 and 2R01AR054458 and a grant from the Eunice Kennedy Shriver National Institute of Child Health and Human Development (NICHD), grant number R01 HD081123-01A1. Kai Li thanks the Agency for Science, Technology and Research (A*STAR, Singapore) for financial support via A*STAR International Fellowship.

References

1. Siegel RL, et al. Cancer statistics. 2016. CA Cancer J Clin. 2016; 66:7–30. [PubMed: 26742998]
2. Ahmed M, et al. Novel techniques for sentinel lymph node biopsy in breast cancer: a systematic review. Lancet Oncol. 2014; 15:e351–362. [PubMed: 24988938]
3. Motomura K, et al. Superparamagnetic iron oxide-enhanced MRI at 3T for accurate axillary staging in breast cancer. Br J Surg. 2016; 103:60–69. [PubMed: 26572241]
4. Harisinghani MG, et al. Noninvasive detection of clinically occult lymph-node metastases in prostate cancer. N Engl J Med. 2003; 348:2491–2499. [PubMed: 12815134]
5. Klenk C, et al. Ionising radiation-free whole-body MRI versus (18)F-fluorodeoxyglucose PET/CT scans for children and young adults with cancer: a prospective, non-tandomised, single-centre study. Lancet Oncol. 2014; 15:275–285. [PubMed: 24559803]
6. Daldrup-Link HE, et al. MRI of tumor-associated macrophages with clinically applicable iron oxide nanoparticles. Clin Cancer Res. 2011; 17:5695–56704. [PubMed: 21791632]
7. Lee N, et al. Water-dispersible ferromagnetic iron oxide nanocubes with extremely high r2 relaxivity for highly sensitive in vivo MRI of tumors. Nano Lett. 2012; 12:3127–3131. [PubMed: 22575047]
8. Singh A, Sahoo SK. Magnetic nanoparticles: a novel platform for cancer theranostics. Drug Discov Today. 2014; 19:474–481. [PubMed: 24140592]
9. Matsumura Y, Maeda H. A new concept for macromolecular therapeutics in cancer chemotherapy: mechanism of tumoritropic accumulation of proteins and the antitumor agent smancs. Cancer Res. 1986; 46:6387–6392. [PubMed: 2946403]
10. Li K, et al. Conjugated polymer based nanoparticle as a dual-modal probe for targeted in vivo fluorescence and magnetic resonance imaging. Adv Funct Mater. 2012; 22:3107–3115.
11. Maeda H, et al. A retrospective 30 years after discovery of the enhanced permeability and retention effect of solid tumors: next-generation chemotherapeutics and photodynamic therapy-problems, solutions, and prospects. Microcirculation. 2016; 23:173–182. [PubMed: 26237291]
12. Xie J, et al. Surface-engineered magnetic nanoparticle platforms for cancer imaging and therapy. Acc Chem Res. 2011; 44:883–892. [PubMed: 21548618]
13. Ahmed N, et al. Theranostic applications of nanoparticles in cancer. Drug Discov Today. 2012; 17:928–934. [PubMed: 22484464]

14. McCarthy JR, Weissleder R. Multifunctional magnetic nanoparticles for targeted imaging and therapy. Adv Drug Deliv Rev. 2008; 60:1241–1251. [PubMed: 18508157]
15. Tassa C, et al. Dextran-coated iron oxide nanoparticles: a versatile platform for targeted molecular imaging, molecular diagnostics, and therapy. Acc Chem Res. 2011; 44:842–852. [PubMed: 21661727]
16. Revia RA, Zhang M. Magnetite nanoparticles for cancer diagnosis, treatment, and treatment monitoring: recent advances. Mater Today. 2016; 19:157–168.
17. Ulbrich K, et al. Targeted drug delivery with polymers and magnetic nanoparticles: covalent and noncovalent approaches, release control, and clinical studies. Chem Rev. 2016; 116:5338–5431. [PubMed: 27109701]
18. Li Z, et al. A smart nanoassembly for multistage targeted drug delivery and magnetic resonance imaging. Adv Funct Mater. 2014; 24:3612–3620.
19. Fang JH, et al. Magnetic core-shell nanocapsules with dual-targeting capabilities and co-delivery of multiple drugs to treat brain gliomas. Adv Healthcare Mater. 2014; 3:1250–1260.
20. Daldrup-Link HE, et al. Alk5 inhibition increases delivery of macromolecular and protein-bound contrast agents to tumors. JCI Insight. 2016; 1:e85608. [PubMed: 27182558]
21. Yin T, et al. Superparamagnetic Fe_3O_4-PEG_{2k}-FA@Ce6 Nanoprobes for in vivo dual-mode imaging and targeted photodynamic therapy. Sci Rep. 2016; 6:36187. [PubMed: 27824072]
22. Zhang L, et al. Phosphatidylserine-targeted bimodal liposomal nanoparticles for in vivo imaging of breast cancer in mice. J Control Release. 2014; 183:114–123. [PubMed: 24698945]
23. Mura SJ, et al. Stimuli-responsive nanocarriers for drug delivery. Nat Mater. 2013; 12:991–1003. [PubMed: 24150417]
24. Zhou H, et al. IGF1 receptor targeted theranostic nanoparticles for targeted and image-guided therapy of pancreatic cancer. ACS Nano. 2015; 9:7976–7991. [PubMed: 26242412]
25. Zhang Y, et al. Cisplatin-loaded polymer/magnetite composite nanoparticles as multifunctional therapeutic nanomedicine. Chinese J Polym Sci. 2014; 32:1329–1337.
26. Vivek R, et al. HER2 targeted breast cancer therapy with switchable “off/on” multifunctional “smart” magnetic polymer core-shell nanocomposites. ACS Appl Mater Interfaces. 2016; 8:2262–2279. [PubMed: 26771508]
27. Makadia HK, Siegel SJ. Poly lactic-co-glycolic acid (PLGA) as biodegradable controlled drug delivery carrier. Polymers (Basel). 2011; 3:1377–1397. [PubMed: 22577513]
28. Wang H, et al. Magnetic/NIR-thermally responsive hybrid nanogels for optical temperature sensing, tumor cell imaging and triggered drug release. Nanoscale. 2014; 6:13001–13011. [PubMed: 25243783]
29. Shen B, et al. Smart multifunctional magnetic nanoparticle-based drug delivery system for cancer thermo-chemotherapy and intracellular imaging. ACS Appl Mater Interfaces. 2016; 8:24502–24508. [PubMed: 27573061]
30. Mehtani S, et al. In vivo expression of an alternatively spliced human tumor message that encodes a truncated form of cathepsin B. Subcellular distribution of the truncated enzyme in COS cells. J Biol Chem. 1998; 273:13236–13244. [PubMed: 9582368]
31. Lin J, et al. Drug/dye-loaded, multifunctional PEG-chitosan-iron oxide nanocomposites for methotrexate synergistically self-targeted cancer therapy and dual model imaging. ACS Appl Mater Interfaces. 2015; 7:11908–11920. [PubMed: 25978458]
32. Ansari C, et al. Development of novel tumor-targeted theranostic nanoparticles activated by membrane-type matrix metalloproteinases for combined cancer magnetic resonance imaging and therapy. Small. 2014; 10:566–575. [PubMed: 24038954]
33. Zanganeh S, et al. Iron oxide nanoparticles inhibit tumour growth by inducing pro-inflammatory macrophage polarization in tumor tissues. Nat Nanotechnol. 2016; 11:986–995. [PubMed: 27668795]
34. Llovet JM, Bruix J. Molecular targeted therapies in hepatocellular carcinoma. Hepatology. 2008; 48:1312–1327. [PubMed: 18821591]
35. Motzer RJ, et al. Lenvatinib, everolimus, and the combination in patients with metastatic renal cell carcinoma: a randomized, phase 2, open-label, multicenter trial. Lancet Oncol. 2015; 16:1473–1482. [PubMed: 26482279]

36. Roth JA, Cristiano RJ. Gene therapy for cancer: what have we done and where are we going? JNCI J Natl Cancer Inst. 1997; 89:21–39. [PubMed: 8978404]
37. Tzeng SY, et al. Polymeric nanoparticle-based delivery of TRAIL DNA for cancer-specific killing. Bioeng Transl Med. 2016; 1:149–159. [PubMed: 28349127]
38. Jin G, et al. Multifunctional organic nanoparticles with aggregation-induced emission characteristics for targeted photodynamic therapy and RNA interference therapy. Chem Commun. 2016; 52:2752–2755.
39. Kim SH, et al. Local and systemic delivery of VEGF siRNA using polyelectrolyte complex micelles for effective treatment of cancer. J Control Release. 2008; 129:107–116. [PubMed: 18486981]
40. Yoo B, et al. Design of nanodrugs for miRNA targeting in tumor cells (13-510-R). J Biomed Nanotechnol. 2014; 10:1114–1122. [PubMed: 24749405]
41. Wang K, et al. Iron-oxide-based nanovector for tumor targeted siRNA delivery in an orthotopic hepatocellular carcinoma xenograft mouse model. Small. 2016; 12:477–48742. [PubMed: 26641029]
42. Hernández-Gil J, et al. An iron oxide nanocarrier loaded with a Pt(IV) prodrug and immunostimulatory dsRNA for combining complementary cancer killing effects. Adv Healthcare Mater. 2015; 4:1034–1042.
43. Joyner MJ, et al. What happens when underperforming big ideas in research become entrenched? JAMA. 2016; 316:1355–1356. [PubMed: 27467098]
44. Le Tourneau C, et al. Molecularly targeted therapy based on tumour molecular profiling versus conventional therapy for advanced cancer (SHIVA): a multicenter, open-label, proof-of-concept, randomized, controlled phase 2 trial. Lancet Oncol. 2015; 16:1324–1334. [PubMed: 26342236]
45. NCI-molecular analysis for therapy choice (NCI-MATCH) trial. https://www.cancer.gov/about-cancer/treatment/clinical-trials/nci-supported/nci-match
46. Huang L, et al. Magneto-plasmonic nanocapsules for multimodal-imaging and magnetically guided combination cancer therapy. Chem Mater. 2016; 28:5896–5904.
47. Yang K, et al. Multimodal imaging guided photothermal therapy using functionalized graphene nanosheets anchored with magnetic nanoparticles. Adv Mater. 2012; 24:1868–1872. [PubMed: 22378564]
48. Zhang M, et al. A multifunctional nanoparticulate theranostic system with simultaneous chemotherapeutic, photothermal therapeutic, and MRI contrast capabilities. RSC Adv. 2016; 6:27798–27806.
49. Hu Y, et al. Multifunctional Fe_3O_4@Au core/shell nanostars: a unique platform for multimode imaging and photothermal therapy of tumors. Sci Rep. 2016; 6:28325. [PubMed: 27325015]
50. Hu Y, et al. Multifunctional pDNA-conjugated polycationic Au nanorod-coated Fe_3O_4 hierarchical nanocomposites for trimodal imaging and combined photothermal/gene therapy. Small. 2016; 12:2459–2468. [PubMed: 26996155]
51. Li K, Liu B. Polymer-encapsulated organic nanoparticles for fluorescence and photoacoustic imaging. Chem Soc Rev. 2014; 43:6570–6597. [PubMed: 24792930]
52. Song X, et al. Ultra-small iron oxide doped polypyrrole nanoparticles for in vivo multimodal imaging guided photothermal therapy. Adv Funct Mater. 2014; 24:1194–1201.
53. Wang C, et al. Iron oxide@polypyrrole nanoparticles as a multifunctional drug carrier for remotely controlled cancer therapy with synergistic antitumor effect. ACS Nano. 2013; 7:6782–6795. [PubMed: 23822176]
54. Liu XM, et al. In vivo 808 nm image-guided photodynamic therapy based on an upconversion theranostic nanoplatform. Nanoscale. 2015; 7:14914–14923. [PubMed: 26300064]
55. Wang D, et al. Targeted iron-oxide nanoparticle for photodynamic therapy and imaging of head and neck cancer. ACS Nano. 2014; 8:6620–6632. [PubMed: 24923902]
56. Wang C, et al. Multifunctional theranostic red blood cells for magnetic-field-enhanced in vivo combination therapy of cancer. Adv Mater. 2014; 26:4794–4802. [PubMed: 24838472]
57. Issels RD. Hyperthermia adds to chemotherapy. Eur J Cancer. 2008; 44:2546–2554. [PubMed: 18789678]

58. Sakaguchi Y, et al. Apoptosis in tumors and normal tissues induced by whole body hyperthermia in rats. Cancer Res. 1995; 55:5459–5464. [PubMed: 7585616]

59. Bettaieb, A., et al. Hyperthermia: cancer treatment and beyond. In: Rangel, L., editor. Cancer treatment-conventional and innovative approaches. InTech; 2013.

60. Quinto CA, et al. Multifunctional superparamagnetic iron oxide nanoparticles for combined chemotherapy and hyperthermia cancer treatment. Nanoscale. 2015; 7:12728–12736. [PubMed: 26154916]

61. Zhou J, et al. Multifunctional Fe_2O_3@PPy-PEG nanocomposite for combination cancer therapy with MR imaging. Nanotechnol. 2015; 26:425101.

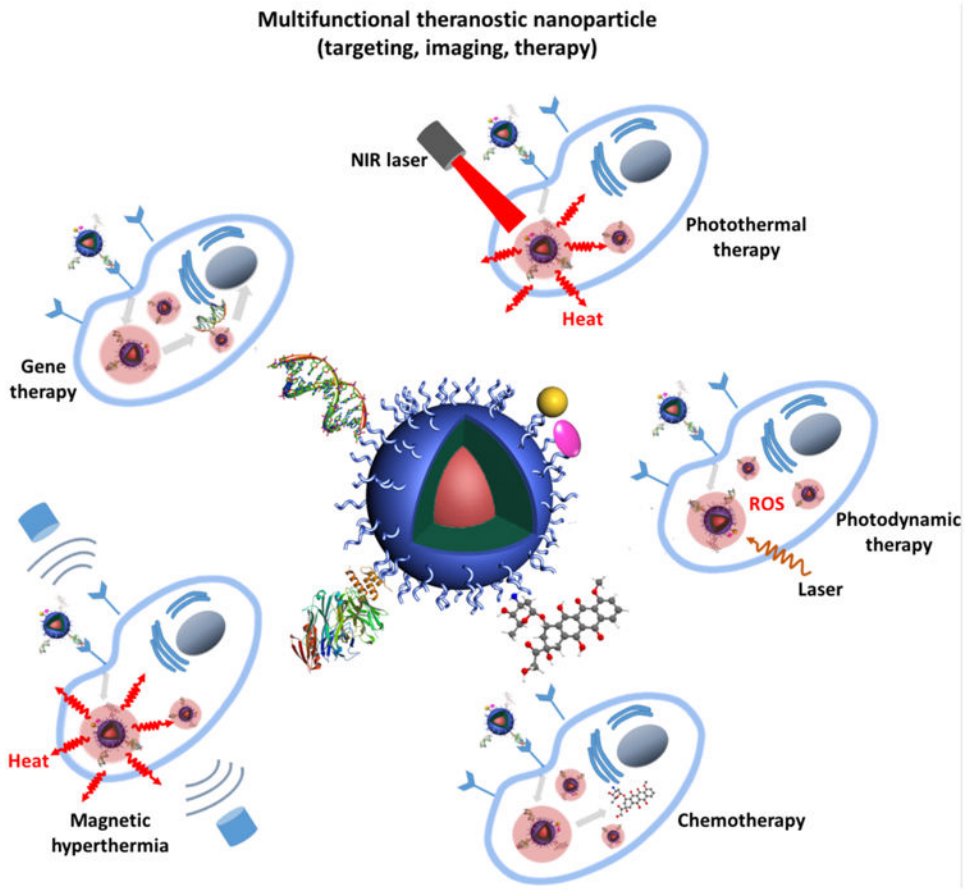

Figure 1.

Schematic illustration of multifunctional SPIO for cancer theranostics. The chemotherapeutics, gene therapeutics, photothermal/photodynamic therapeutics, fluorescent moieties and targeting moieties can be incorporated to the polymer coating through different strategies.

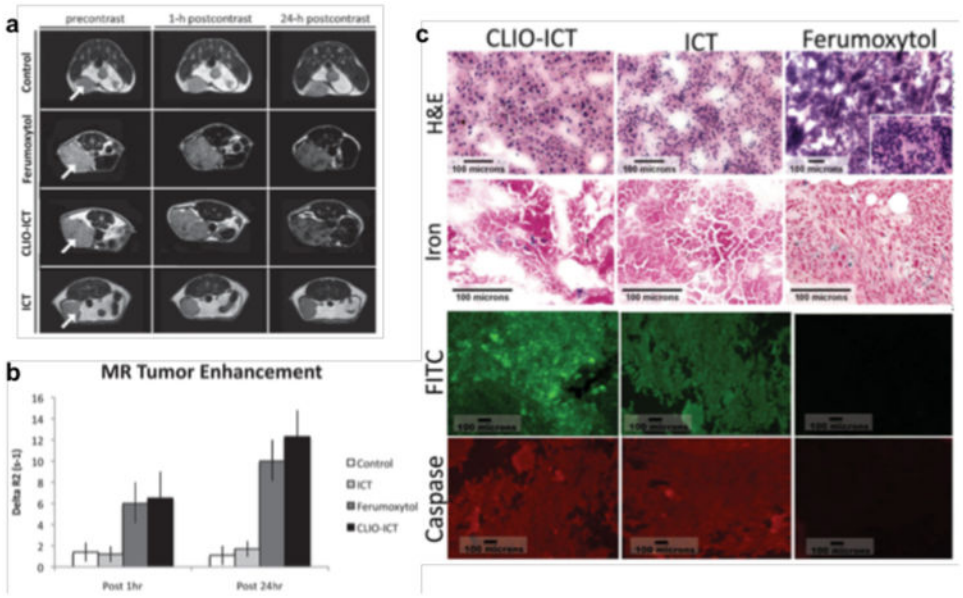

Figure 2.

(a) Axial T_2-weighted MR images (TR 2500 ms, TE 80 ms) of MMTV-PyMT mammary tumors before and after a single intravenous injection of different components. (b) MR signal enhancement data in tumors quantified as $\Delta R_2 = (R_2\text{pre} - R_2\text{post})$. (c) Cell death in MMTV-PyMT tumors. H&E panels: CLIO-ICT treated tumor demonstrating diffuse necrosis; ICT treated tumor with predominately viable tumor cells and a subset of cells undergoing necrosis; Ferumoxytol treated tumor with diffuse viability and no necrosis. Iron panels: Scattered CLIO-ICT treated tumor and rare admixed histiocytes contain blue pigment indicating cytoplasmic iron deposition; ICT treated tumor shows no cytoplasmic iron deposition, scattered iron laden histiocytes serve as an internal positive control; Ferumoxytol treated tumor show cytoplasmic iron deposition, scattered iron laden histiocytiocytes serve as an internal positive control. FITC panels: Fluorescence microscopy showing FITC signal for CLIO-ICT and ICT but no signal for Ferumoxytol. Caspase-3 panels: CLIO-ICT and ICT treated tumors show Cy3 labeling throughout the samples; Ferumoxytol treated tumor shows few areas with weak Cy3 fluorescence. Reprinted with permission from WILEY-VCH Verlag GmbH & Co. KGaA, Weinheim [32].

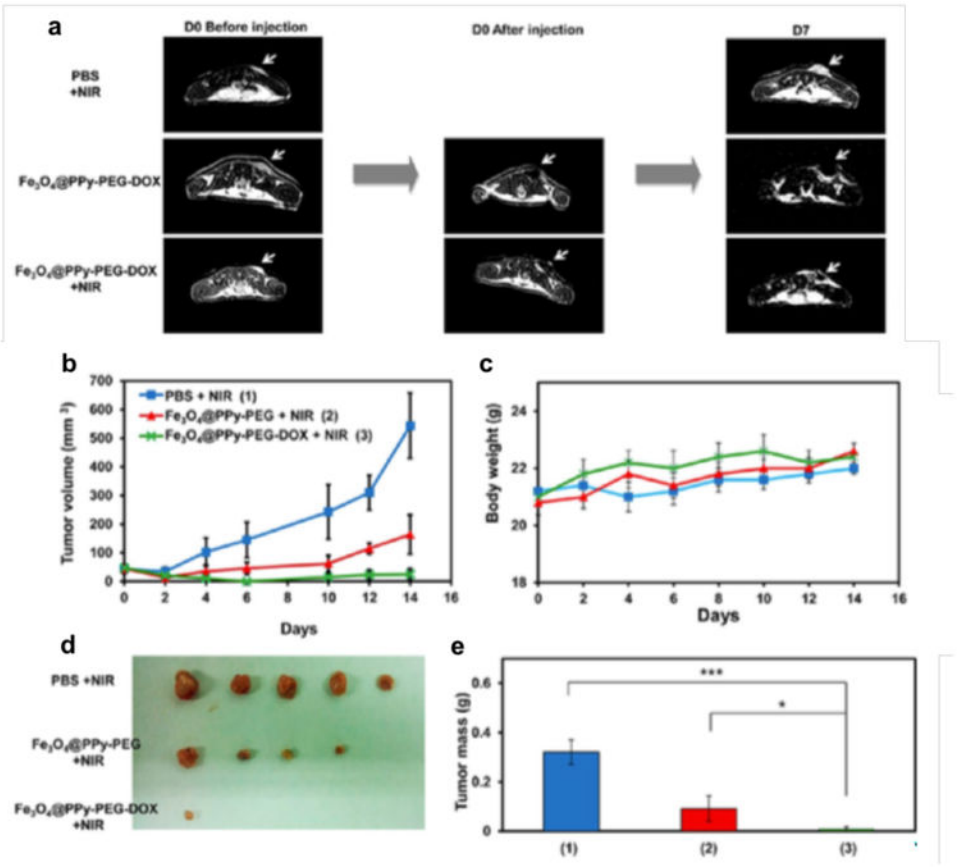

Figure 3.

(a) Representative MR images of mice from three different groups obtained at day 0 before and after injection and day 7 after treatment (tumors marked by the white arrow). (b) Tumor growth curves of different groups of mice after various treatments indicated (n = 5). (c) Body weights of mice after various treatments indicated. (d) Photos of the tumors collected from different groups of mice at day 14. (e) Average weights of tumors collected from mice at the end of various treatments indicated. Error bars are based on SEM (***p < 0.001, **p < 0.01, or *p < 0.05, by ANOVA with Tukey's post-test). Reprinted with permission from American Chemical Society [53].

Drug Discov Today. Author manuscript; available in PMC 2018 September 01.

Table 1

Multifunctional theranostic SPIONs for cancer imaging and therapy

Polymer Coating	Size (nm)	Imaging Modality	Therapy Modality	Targeting Ligands	Application
Chitosan	-	MRI	Chemotherapy (camptothecin)	Folate	*In vivo* magnet-guided MRI and treatment for Kunming mice bearing H22 tumor [18]
Polyvinyl alcohol/polyacrylic acid	100-150	MR/fluorescence imaging	Chemotherapy (doxorubicin and curcumin)	Lactoferrin	*In vivo* magnet-guided fluorescence imaging and treatment for BALB/c nude mice bearing RG2 glioma tumor [19]
Amphiphilic polymer (undefined)	20	MR/fluorescence imaging	Chemotherapy (doxorubicin)	IGF1 peptide	*In vivo* targeted MR/fluorescence imaging and treatment for nude mice bearing orthotopic pancreatic patient-derived xenograft tumor [24]
PLGA	80-100	MR/fluorescence imaging	Chemotherapy (tamoxifen)	Herceptin	*In vitro* test for pH-/thermal-responsive drug release and *in vivo* chemotherapy for MCF-7 tumor treatment [26]
PNIPAM copolymer	170	MR/fluorescence imaging	Chemotherapy (curcumin)	None	*In vitro* temperature sensing and temperature-responsive drug release with NIR irradiation or AMF [28]
PNIPAM	370-430	MR/fluorescence imaging	Chemotherapy (5-fluorouracil)	None	*In vitro* thermal-responsive drug release for 7901 cell treatment [29]
PEG/chitosan	52	MR/fluorescence imaging	Chemotherapy (methotrexate)	Methotrexate (mimic folate)	*In vivo* targeted MR and fluorescence imaging with protease-mediated drug release to inhibit Hela tumor growth in Sprague-Dawley rats [31]
Dextran	21	MR/fluorescence imaging	Chemotherapy (azademethylcolchicine)	None	*In vivo* MRI and targeted drug activation in MMP-14 expressed MMTV-PyMT tumor with low toxicity to normal tissue of FvBN mice [32]
Chitosan-PEG grafted PEI	41	MRI	Gene therapy (siRNA)	Anti-GPC3 Ab	*In vivo* targeted delivery of siRNA for orthotopic HCC therapy in athymic Nu/J mice [41]
Phospholipid-PEG	45-50	MRI	Immunotherapy (dsRNA analog); Chemotherapy {Pt(IV)}	None	*In vitro* evaluation for combined chemoimmunotherapy for cancer treatment [42]
PEO-*b*-PCL	190	MRI	PTT (Au); Chemotherapy (paclitaxel)	None	*In vitro* test of combined chemotherapy and PTT to MCF-7 and MDA-MB-231 cells [48]
PEI/PEG	150	MRI/CT/PAI	PTT (Au)	Folate	*In vivo* trimodal imaging and PTT treatment for Hela tumors [49]

Polymer Coating	Size (nm)	Imaging Modality	Therapy Modality	Targeting Ligands	Application
PDA/PDM	210	MRI/CT/PAI	Gene therapy (plasmid DNA); PTT (Au)	None	*In vivo* trimodal imaging and PTT/genetherapy for C6 glioma tumor-bearing BALB/c nude mice [50]
PEG/PPy	100	MRI/PAI	PTT (PPy)	None	*In vivo* MRI/PAI and PTT treatment for BALB/c nude mice bearing 4T1 tumor [52]
C18PMH-PEG	100	MRI	PTT (PPy) Chemotherapy (doxorubicin)	None	*In vivo* MRI and chemotherap/PTT treatment for BALB/c nude mice bearing 4T1 tumors [53]
PEG	14-18	MR/fluorescence imaging	PDT (Ce6); Chemotherapy (doxorubicin)	Red blood cell	*In vivo* MR and fluorescence imaging and chemotherapy/PDT to suppress 4T1 tumor growth in BALB/c nude mice [56]
Phospholipid-PEG	28-30	MRI	Hyperthermia (SPION); Chemotherapy (doxorubicin)	None	*In vitro* study of combined hyperthermia and chemotherapy to Hela cells [60]
PEG/PPy	153	MRI	Hyperthermia (SPION); Chemotherapy (doxorubicin)	None	*In vivo* MRI and combined hyperthermia/chemotherapy to control HepG2 tumor growth in nude mice [61]